Characterization of Highly Dispersive Materials Using Composite Coaxial Cells: Electromagnetic Analysis and Wideband Measurement

Jifu Huang, Ke Wu, *Senior Member, IEEE*, Patrick Morin, and Cevdet Akyel, *Member, IEEE*

Abstract—**In this work, theoretical modeling and experimental characterization of composite coaxial-line cells are made for accurate dielectric measurement. The coaxial cells are designed such that highly dispersive materials can be characterized over a wide band of frequencies. In addition, a transmission line matrix (TLM) algorithm with a new type of node is proposed for electromagnetic analysis of the complex composite geometry of the measurement cells. Such a hybrid-mode simulation allows the electrical performance of the proposed cells to be determined for a variety of complex permittivity measurements. The proposed node in the cylindrical coordinate not only accommodates cylindrical coaxial discontinuities in the cell, but also describes the frequency-dependent properties of material. Experiments on a network analyzer were done with a number of APC-7 coaxial cells and various liquid samples to verify the wideband characteristics of the technique. It is found both theoretically and experimentally that the sample volume can be adjusted to ensure a wideband sensibility of the S-parameters. A sensitivity factor is also defined to characterize the frequency response of the coaxial cells. Such an electromagnetic analysis (direct problem) can be used in extracting unknown dielectric characteristics of a material (inverse problem) based on a recently proposed generic approach.**

I. Introduction

It is well known that wideband measurements of highly dispersive materials are extremely useful in the study of electromagnetic energy absorption [1]–[4]. Precise parameter extraction of dielectric permittivity is usually achieved using a resonant-cavity technique which is limited to, unfortunately, single-frequency or narrow-band measurements. The coaxial-line technique [5] has demonstrated unmatched advantages compared to other approaches. This is mainly attributed to its high measurement sensitivity, wideband TEM propagation and simple mechanical assembly. Similar to the rectangular waveguide technique, the coaxial-line technique presents no radiation or leaky losses and offers therefore a highly precise measurement if the system is well calibrated and characterized.

A coaxial measurement cell usually consists of a specifically shaped composite geometry partially filled with a material sample. In this work, a new wideband measurement technique is proposed for accurate extraction of complex permittivity using a coaxial discontinuity. The material under measurement may be in the form of liquid or powder. As is shown in Fig. 1, the sample occupies the outer space near the inner face of cylindrical conductor. In this way, a high sensitivity over a wide band of frequencies can be achieved by choosing an appropriate filling factor of the material with respect to the whole cell, thereby controlling the degree of interaction between electromagnetic field and the sample. Even if a very conductive (or highly absorptive) material is considered, the transmission coefficient can be still measurable as long as the coaxial cell is properly designed. Therefore, a thorough knowledge of wave propagation and scattering along the coaxial cell is mandatory in understanding the working mechanism and parametric dependence of the electrical characteristics. This is also important for the design of an optimized wideband coaxial-line cell. Obviously, an accurate electromagnetic analysis of the composite coaxial-line cell involving a variety of materials should be deployed to predict the frequency-dependent electrical performance as well as its parametric dependence of geometry.

A recently developed field-theory-based technique called the frequency-domain transmission line matrix (FDTLM) method is used to analyze and characterize the proposed composite coaxial-line cell for wideband measurements. In particular, a new frequency domain symmetrical condensed node (FDSCN) is developed to model a general dispersive medium. Subsequently, a unified approach [6], [7] is applied to calculate the S-parameters. Knowing *a priori* the complex permittivity of a dielectric, a set of generic diagrams [8] can be established to interrelate intrinsically the S-parameters and complex permittivity. As a result, the unknown dielectric permittivity can be determined from these diagrams when considered together with an S-parameter measurement. It is shown that numerical techniques are very useful in the material measurement for both direct and inverse problems. A variety of experiments are also carried out to verify the theoretical predictions and electrical performance of the proposed coaxial cells.

II. Theoretical Modeling

Although the FDTLM provides a unified algorithm to tackle complex electromagnetic modeling, the well established ana-

Manuscript received September 16, 1995; revised January 17, 1996. This work was supported by the Natural Sciences and Engineering Research Council (NSERC) of Canada.

The authors are with POLY-GRAMES Research Center, Department de Génie Électrique et de Génie Informatique, École Polytechnique, C. P. 6079, Succ. Centre-Ville, Montréal H3C 3A7 Canada

Publisher Item Identifier S 0018-9480(96)03030-X.

0018–9480/96$05.00 © 1996 IEEE

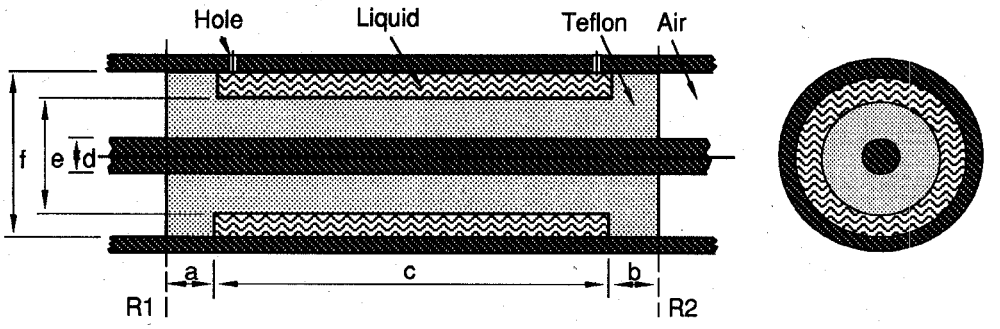

Fig. 1. A wideband composite coaxial cell for dielectric measurement.

lyzes based on the Cartesian coordinate may cause a significant error of discretization when a curved geometry is involved. To this end, a cylindrical coordinate system directly in the frequency-domain is considered in the following formulation to better accommodate the coaxial line geometry although a TLM cylindrical node was proposed in the time-domain [12]. In this way, the error of discretization can be minimized. In this work, a frequency-domain node in the cylindrical coordinate is proposed to describe inherently a dispersive medium to be measured by the coaxial line cell. The details regarding how to calculate the S-parameters has been documented elsewhere [6] ,[7] and is therefore omitted here.

It is well known that the node is the core of the TLM algorithm. In a previous work [9], a simple frequency-domain node was derived to model cylindrical microstrip discontinuities. It is unfortunate that for certain mesh sizes, however, the propagation constant on the cylindrical TLM grids may become zero or even negative. This leads to a undesirable situation of high nodal dispersion and poor spatial resolution. To remedy such a deficiency of the original node, and at the same time, to accommodate a highly lossy dispersive medium in the node, a new version of FDSCN is formulated. The condensed node used in the analysis is depicted in Fig. 2. It can be considered as three shunt and three series elementary nodes that are coupled with each other at the center of the node [13]. This is a primary consideration in the derivation of a condensed node. The admittances of the three series elementary nodes are defined on the basis of the transmission line theory and can be expressed as follows:

$$Y_r = \frac{\Delta_l \Delta_r}{\Delta_\theta \Delta_z}\sqrt{\frac{\sigma_e + j\omega\epsilon_0\epsilon'}{\sigma_m + j\omega\mu_0\mu'}} \tag{1a}$$

$$Y_\theta = \frac{\Delta_l \Delta_\theta}{\Delta_r \Delta_z}\sqrt{\frac{\sigma_e + j\omega\epsilon_0\epsilon'}{\sigma_m + j\omega\mu_0\mu'}} \tag{1b}$$

$$Y_z = \frac{\Delta_l \Delta_z}{\Delta_\theta \Delta_r}\sqrt{\frac{\sigma_e + j\omega\epsilon_0\epsilon'}{\sigma_m + j\omega\mu_0\mu'}} \tag{1c}$$

in which $\Delta_l = \sqrt{(\Delta_r^2\Delta_\theta^2 + \Delta_r^2\Delta_z^2 + \Delta_\theta^2\Delta_z^2)/(\Delta_r^2 + \Delta_\theta^2 + \Delta_z^2)}$. Y_r is associated with the r-oriented series node including link lines 4, 5, 7, and 8; $Y_\theta$is associated with the θ-oriented series node including link lines 2, 6, 9, and 10; and Y_z is associated with the z-oriented series node including link lines 1, 3, 11, and 12. The symbols Δ_r, Δ_θ, and Δ_z denote the dimensions of the node. The conductivity is defined as $\sigma_m = \omega\mu_0\mu''$ and $\sigma_e = \sigma_s + \omega\epsilon_0\epsilon''$. σ_s is the static electrical conductivity, and $\epsilon', \epsilon'', \mu'$, and μ'' may be frequency-dependent.

A 12×12 scattering matrix is derived in a way similar to that of the time-domain TLM formalism [10], [11]. The connection of the link lines at the nodal center is governed by a voltage scattering matrix S_c such as

$$V^r = S_c \cdot V^i \tag{2}$$

where

$$V^{i,r} = (V_1^{i,r}, V_2^{i,r}, \cdots, V_{12}^{i,r})^T$$

and as in matrix S_c shown at the bottom of the next page.

The elements of the matrix S_c are normally determined by enforcing energy conservation and applying the voltage and current laws for the incident and reflected voltage waves at the center of the node. This yields

$$a_r = \frac{Y_z - Y_\theta}{2(Y_z + Y_\theta)}, \quad b_r = \frac{Y_z}{Y_z + Y_\theta} \tag{3a}$$

$$a_\theta = \frac{Y_z - Y_r}{2(Y_z + Y_r)}, \quad b_\theta = \frac{Y_z}{Y_z + Y_r} \tag{3b}$$

$$a_z = \frac{Y_\theta - Y_r}{2(Y_\theta + Y_r)}, \quad b_z = \frac{Y_\theta}{Y_\theta + Y_r}. \tag{3c}$$

In order to build up the entire FDTLM algorithm, the reference planes have to be moved from the center of the node to its ports. This is equivalent to multiplying the incident and reflected waves by an appropriate phase delay factor such as $\exp(\gamma\Delta)$, where γ is the corresponding propagation constant of the nodal link line and Δ is the mesh size. On the other hand, an analogy [10] can be established between the time-harmonic Maxwell's curl equation, written in terms of field components, and the Telegraph equations governing the propagation characteristics of voltage waves in a transmission-line network. This analogy yields six relations of equivalence that relate complex characteristic impedance and propagation constant of the link lines to local dimensions of the mesh and also properties of the medium to be modeled. Such a procedure

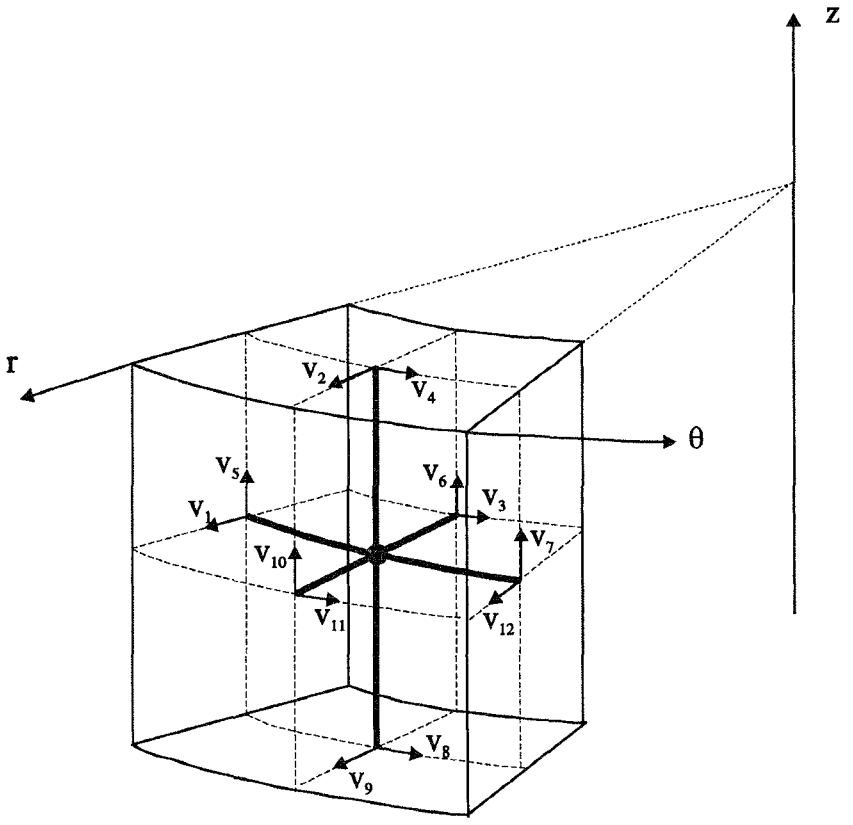

Fig. 2. Symmetrical condensed node in the cylindrical coordinate.

leads to the propagation constants of the link lines

$$\gamma_1 = \frac{\Delta_l \Delta_\theta}{\Delta_r^2 + \Delta_\theta^2} k \tag{4a}$$

$$\gamma_2 = \frac{\Delta_z(\Delta_r^2 + \Delta_\theta^2 - \Delta_l^2)}{\Delta_l(\Delta_r^2 + \Delta_\theta^2)} k \tag{4b}$$

$$\gamma_3 = \frac{\Delta_l \Delta_r}{\Delta_r^2 + \Delta_\theta^2} k \tag{4c}$$

$$\gamma_4 = \frac{\Delta_z(\Delta_r^2 + \Delta_\theta^2 - \Delta_l^2)}{\Delta_l(\Delta_r^2 + \Delta_\theta^2)} k \tag{4d}$$

$$\gamma_5 = \frac{\Delta_\theta \Delta_r^2}{\Delta_l(\Delta_r^2 + \Delta_\theta^2)} k \tag{4e}$$

$$\gamma_6 = \frac{\Delta_r \Delta_\theta^2}{\Delta_l(\Delta_r^2 + \Delta_\theta^2)} k \tag{4f}$$

where k is the intrinsic wave number of the medium inside the node. It is obvious that all above-mentioned propagation constants of the link lines are always multiplied by a positive value with the intrinsic wave number k regardless of the variation of the graded mesh size. At this stage, the voltage waves at the nodal ports can be obtained simply by applying

$$S_c = \begin{array}{c|c} & \begin{array}{cccccccccccc} 1 & 2 & 3 & 4 & 5 & 6 & 7 & 8 & 9 & 10 & 11 & 12 \end{array} \\ \hline \begin{array}{c} 1 \\ 2 \\ 3 \\ 4 \\ 5 \\ 6 \\ 7 \\ 8 \\ 9 \\ 10 \\ 11 \\ 12 \end{array} & \begin{pmatrix} a_r & 1-b_r & 0.5 & & & & & & 1-b_r & & -0.5 & a_r \\ b_r & -a_r & & & & 0.5 & & & -a_r & -0.5 & & b_r \\ 0.5 & & a_\theta & 1-b_\theta & & & & 1-b_\theta & & & a_\theta & -0.5 \\ & & b_\theta & -a_\theta & 0.5 & & -0.5 & -a_\theta & & & b_\theta & \\ & & & 0.5 & -a_z & b_z & -a_z & -0.5 & & b_z & & \\ & 0.5 & & & 1-b_z & a_z & 1-b_z & & -0.5 & a_z & & \\ & & & -0.5 & -a_z & b_z & -a_z & 0.5 & & b_z & & \\ & & b_\theta & -a_\theta & -0.5 & & -0.5 & -a_\theta & & & b_\theta & \\ b_r & -a_r & & & & -0.5 & & & -a_r & 0.5 & & b_r \\ & -0.5 & & & 1-b_z & a_z & 1-b_z & & 0.5 & a_z & & \\ -0.5 & & a_\theta & 1-b_\theta & & & & 1-b_\theta & & & a_\theta & 0.5 \\ a_r & 1-b_r & -0.5 & & & & & & 1-b_r & & 0.5 & a_r \end{pmatrix} \end{array}$$

the following transformation:

$$V_p^r = P \cdot S_c \cdot P \cdot V_p^t \tag{5}$$

with (6) as shown at the bottom of the next page.

The modeling of a composite coaxial measurement cell in the present work will inevitably deal with the simulation of an interface between two different dielectric media. This can be easily handled by an appropriate nodal interconnection for which transmission and reflection take place [13]. These measures take into account the interfacing effects. Combining the above-described node and the FDTLM algorithm presented in [7], the S-parameters of a coaxial discontinuity cell can be calculated. Compared to other techniques such as the mode-matching method, the present algorithm is very flexible for arbitrary and complex cylindrical structures. In addition, solving the proposed coaxial cell problem that has a certain degree of symmetry, our algorithm is also very fast and efficient. For instance, the calculation of a typical coaxial discontinuity using the present modeling technique for generating a complete figure such as illustrated in Fig. 6 takes approximately five minutes on a HP-715/100 workstation.

III. Measurement Technique

A wideband composite cell (see Fig. 1) was made with a through coaxial-line (copper with a static conductivity $\sigma_s = 5.76 \times 10^7$ S/m) in which the chamber to be filled with a sample material is located near the outer conductor. A Teflon container ($\epsilon' = 2.31, \tan\ \delta = 1 \times 10^{-4}$) is used to hold liquid samples. The influences of loss factor will be accounted for in our model. The injection of a liquid material is done through two holes on the outer conductor. To examine the accuracy of our theoretical modeling, a number of experiments were made for various liquid samples using a network analyzer (HP8510-C) via a APC-7 standard in 1–18 GHz frequency range. A standard two-port calibration was carried out for S-parameter measurements. It is clear that the volume of chamber is controllable. In an effort to obtain a high measurement sensitivity with regards to the geometry of coaxial cell and complex permittivity, a sensitivity factor $\mathcal{R}$ can be defined such that its value indicates when a high-precision material measurement can be determined with the S-parameter technique. This factor is given by

$$\mathcal{R} = |S_{21}|^2 + |S_{11}|^2. \tag{7}$$

Obviously, the sensitivity factor is essentially the normalized power. $\mathcal{R}$ becomes unitary for a lossless material and of course tends to be smaller than 1.0 for lossy material. In this way, the success or failure of a highly dispersive and lossy material is well reflected in the value of $\mathcal{R}$. In other words, whether the precision of a measurement is considered to be acceptable or not can be judged simply by its sensitivity factor. It can be said that a good (or high) precision of measurement can be achieved only if the sensitivity factor is greater than a certain value. We used $\mathcal{R} = 0.2$, for example, as the critical value for a particular measurement cell, although this criterion is totally arbitrary. Nevertheless, the proposed sensitivity factor provides an intuitive way to choose a good measurement cell for experiments. This can be done first by applying field-theoretical modeling which can assess the measurement with a predetermined precision. It can be seen that the defined sensitivity factor is not only frequency-dependent but also related to the geometry (topology) of a particular cell.

Using the proposed TLM algorithm, it is easy to evaluate the quality and precision of a measurement cell for a class of materials by determining the sensitivity factor. Given a known range of material properties to be measured for a frequency band of interest, it is possible to design a particular cell such that its sensitivity factor is greater than the critical value throughout the designated frequency band. Therefore, this procedure is useful for getting the maximum precision possible out of an experimental set-up.

As examples of application, two highly dispersive and lossy liquids (propanol and water) are considered in the frequency range of 1 to 18 GHz. Fig. 3 presents the dispersion characteristics of the complex permittivity of the two liquid samples which were obtained using a HP85070B probe. These data indicate that it would be erroneous to use the conventional analytical formula of ϵ'' in terms of conductivity. This is because, for highly dispersive materials, the imaginary part of the permittivity is not always linearly dependent on conductivity.

Figs. 4 and 5 show frequency-dependent characteristics of the $\mathcal{R}$ factor of two different cells for both propanol and water, respectively. The dimensions of the cells are included in Table I. As indicated clearly in Fig. 4, the electromagnetic

$$P = \begin{pmatrix} e^{-\gamma_1 \Delta_\theta/2} & & & & & & & & & & & & \\ & e^{-\gamma_2 \Delta^z/2} & & & & & & & & & & & \\ & & e^{-\gamma_3 \Delta_r/2} & & & & & & & & & & \\ & & & e^{-\gamma_4 \Delta^z/2} & & & & & & & & & \\ & & & & e^{-\gamma_5 \Delta_\theta/2} & & & & & & & & \\ & & & & & e^{-\gamma_6 \Delta_r/2} & & & & & & & \\ & & & & & & e^{-\gamma_5 \Delta_\theta/2} & & & & & & \\ & & & & & & & e^{-\gamma_4 \Delta_z/2} & & & & & \\ & & & & & & & & e^{-\gamma_2 \Delta_z/2} & & & & \\ & & & & & & & & & e^{-\gamma_6 \Delta_r/2} & & & \\ & & & & & & & & & & e^{-\gamma_3 \Delta_r/2} & & \\ & & & & & & & & & & & e^{-\gamma_1 \Delta_\theta/2}. \end{pmatrix} \tag{6}$$

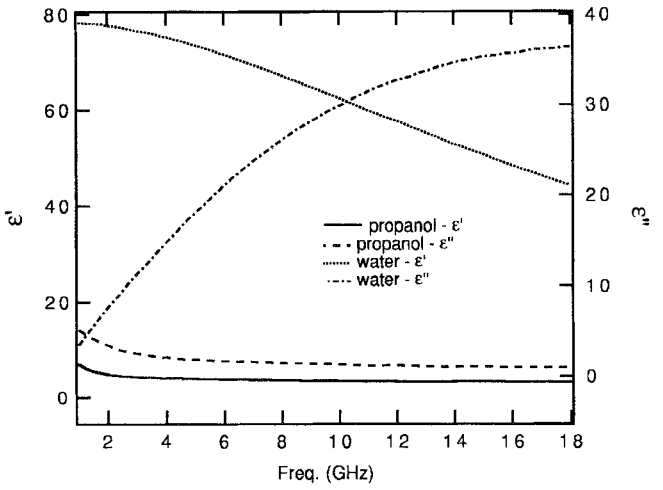

Fig. 3. Complex permittivities of water and propanol as functions of frequency.

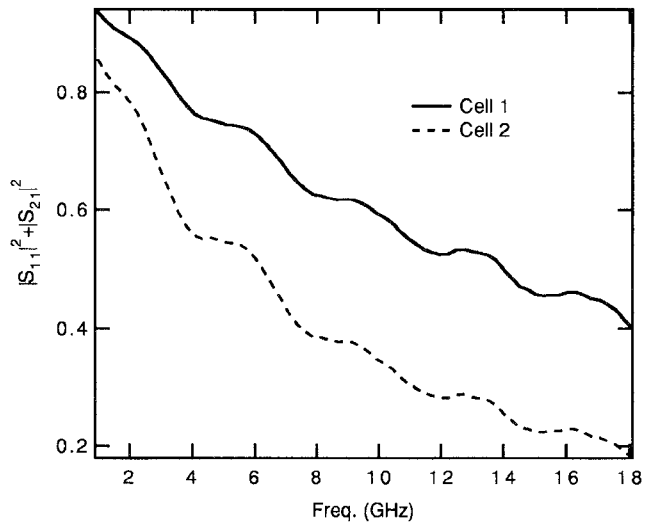

Fig. 4. Frequency-dependent characteristics of the sensitivity factor for cells 1 and 2 described in Table I and filled with a propanol sample.

absorption is less pronounced and a wideband measurement sensitivity using the transmission coefficient can be easily obtained for the relatively low-loss propanol. In this case, both cells 1 and 2 can be used for achieving $\mathcal{R} > 0.2$ over the frequency band of interest. In the case where a relatively high-loss water sample is measured under the room temperature, however, $\mathcal{R}$ tends to be zero at the high end of the frequency band for cell 2 (Fig. 5). This suggests that cell 2 cannot be used, and that cell 3 should be chosen instead for the measurement. Based on these cells, the very good agreement between the theoretical and experimental transmission coefficients shown in Figs. 6 and 7 validates the FDTLM modeling. The minor difference in the results may be attributed to the numerical precision of the algorithm, or to measurement calibration errors, or to both.

IV. Inverse Problem

One of the biggest difficulties encountered in dielectric measurements using a discontinuity of transmission line is the

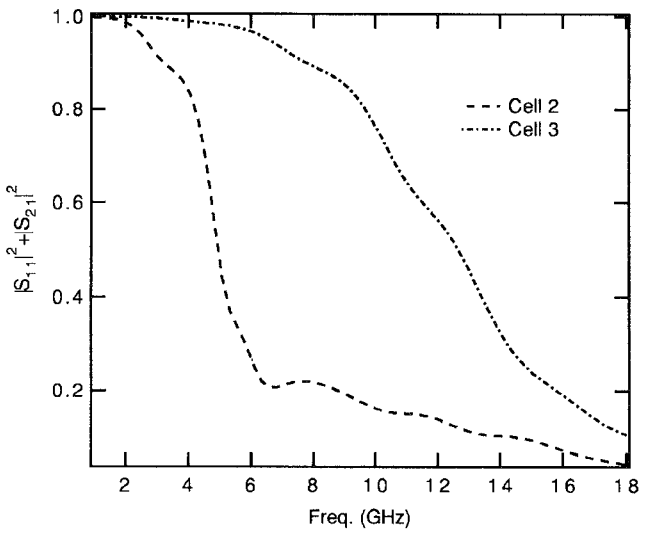

Fig. 5. Frequency-dependent characteristics of the sensitivity factor for cells 2 and 3 described in Table I filled with a water sample.

TABLE I
Geometrical Dimensions of Coaxial Cells
(Refer to Fig. 1, $d = 3.0$ mm, $f = 7.0$ mm)

cell	a	b	c	e
1	2.35	2.99	19.79	5.27
2	2.67	2.57	19.31	4.30
3	2.77	3.01	19.44	6.07
4	2.84	2.64	20.00	6.25
5	2.84	2.64	10.00	6.60

inverse problem. In other words, how complex permittivity can be precisely deduced from the measured transmission and reflection coefficients. So far, most approaches are mainly based on the use of iterative procedures with certain predetermined error criteria [3]–[5]. These approaches may lead to prohibitively long CPU times and convergence problems may also take place. Obviously, such iterative procedures are not useful for real-time or fast dielectric measurement. Very recently, a generic approach [8] has been proposed to bridge the gap between the direct problem and its inverse counterpart. This is done using a simple generic equation that is derived to calculate explicitly the complex permittivity from the measured S-parameters for a small sample volume. This generic technique allows one to exploit field-theoretical numerical techniques for complex-geometry measurement cells for which analytical solutions are not available.

To further extend such a generic approach to dielectric measurements using a coaxial cell, a set of generic diagrams are generated for each frequency point. These diagrams are used to deduce an intrinsic relationship between the calculated S-parameters and complex permittivity. Note that the defined sensitivity factor $\mathcal{R}$ could also be useful for the inverse problem. Nevertheless, this factor is primarily intended to determine the measurement quality for lossy materials over wideband of frequency of interest when a specific geometry of the measurement cell is considered. In the case of considering an inverse problem, $\mathcal{R}$ could be much less involved. This is because a lossless material with a very high permittivity

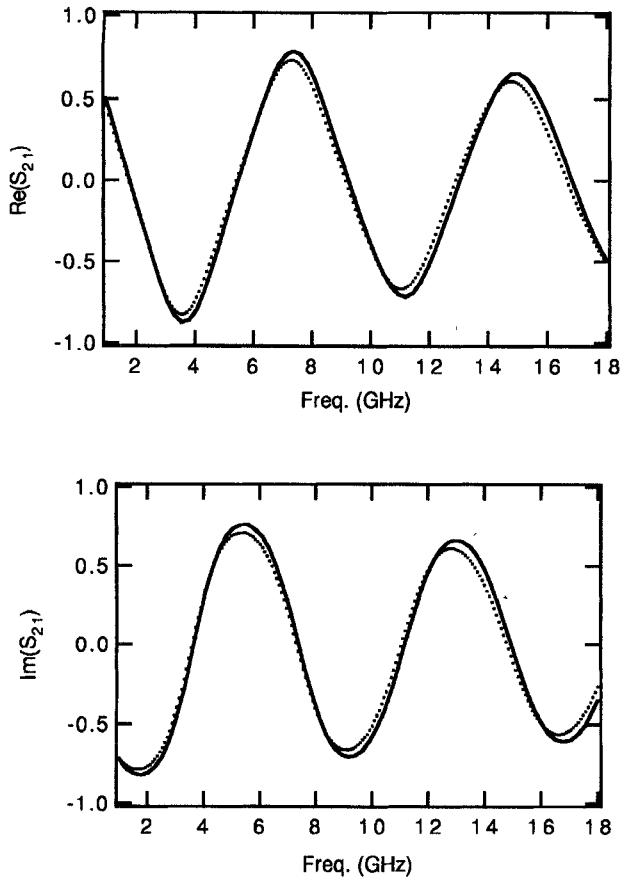

Fig. 6. Comparison of theoretical and measured transmission coefficients for a propanol sample (— theoretical results; ····· experimental results).

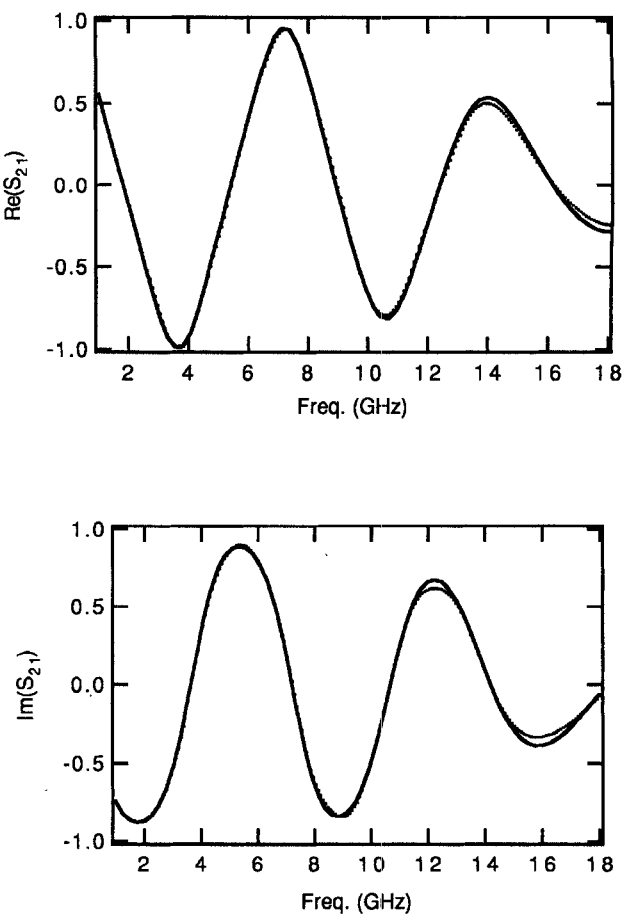

Fig. 7. Comparison of theoretical and measured transmission coefficients for a water sample (— theoretical results; ····· experimental results).

certainly yields the unity sensitivity factor but may have some serious difficulties in the parameter extraction through a S-parameter measurement such as the well known multiple solution. Actually, $\mathcal{R}$ is more and less used to judge the measurement quality of cell as long as the direct problem is concerned. In the inverse procedure, this factor should not be of primary concern. Therefore, $\mathcal{R}$ will be ignored in the following analysis and discussion.

It is found that, if the cell 4 is selected for measurement, its scattering parameter S_{21} is a single-valued function of complex permittivity when the imaginary part of permittivity is smaller than 25, as shown in Fig. 8. In other words, there is a one-to-one mapping between the S-parameter and complex permittivity for low- and medium-loss materials at a particular frequency. This is also to say that extra care should be taken in the case of very high-loss samples, for example, larger than 25 in our case study, for which multiple-valued characteristic functions may appear in generic diagrams. Thus, the complex permittivity ϵ' and ϵ'' can be traced down from the look-up graphs once S_{21} is measured for a unknown material sample. There is a possibility of expanding the single-valued range of complex permittivity for high-loss materials such as water simply by compressing the volume of the measurement chamber. This can be easily done by reducing, for example, the thickness and length of cell. Cell 5 was made for such a study, and we found that the single-valued imaginary part of permittivity was extended well beyond 100,

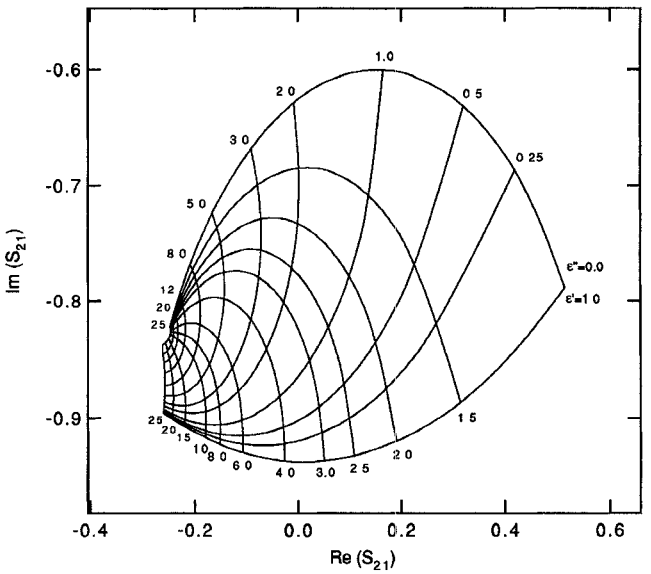

Fig. 8. A generic diagram showing the variation of complex permittivity versus the S-parameter S_{21} in the complex plane at 10 GHz for coaxial cell 4.

as shown in Fig. 9. It is noted, however, that a small sample volume may lead to a lower measurement sensitivity and complicated mechanical processing. As such, there is a trade-

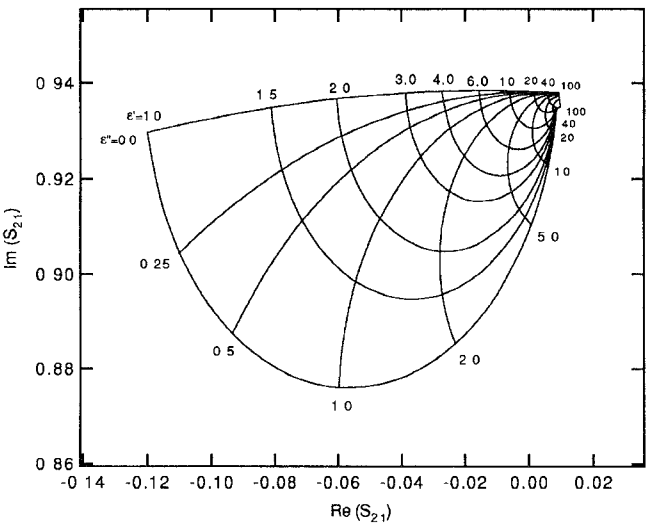

Fig. 9. A generic diagram showing the variation of complex permittivity versus the S-parameter S_{21} in the complex plane at 10 GHz for the coaxial cell 5

TABLE II
MEASURED AND EXTRACTED COMPLEX PERMITTIVITIES OF A METHANOL SAMPLE FOR SEVERAL FREQUENCY POINTS USING CELL 4 IN TABLE I

F (GHz)	S_{21}	Generic diagram		Measurement	
		ε'	ε''	ε'	ε''
1	0.624-j0.719	30.90	7.15	30.89	7.13
5	-0.541+j0.759	13.60	12.90	13.58	12.93
10	-0.199-j0.835	7.80	8.50	7.79	8.51
15	0.740+j0.372	6.50	6.10	6.52	6.07
18	-0.298-j0.712	6.20	5.30	6.18	5.31

off in choosing an appropriate geometry for an optimized wideband characterization of a material.

To test the effectiveness of the proposed generic diagrams, a methanol sample was injected into the chamber of the cell 4, and a set of S-parameters ware measured. Then the complex permittivity was determined from the corresponding generic look-up diagrams for each frequency. Table II gives the resulting complex permittivity for methanol, which compares well with additional experimental results obtained using the HP85070B probe. This confirms the validity of the generic approach.

V. CONCLUSION

A generalized TLM algorithm for cylindrical coordinates is proposed in this paper for material characterization in the frequency domain using a coaxial-line cell. The proposed characterization technique using a composite coaxial through-line promises wideband measurement sensitivity, which is well confirmed by the theoretical prediction. This coaxial cell is particularly suitable for a large class of highly dispersive liquid and powder materials. A sensitivity factor is defined in this work to quantitatively characterize the quality and measurement precision of such a coaxial cell. It is shown that the inverse characterization can be easily done by using a generic approach based on this numerical technique (the direct problem) combined with experimental calibrations. The problem related to achieving single-valued functions of complex permittivity in the generic diagrams is discussed with examples. Very good agreement between the theory and measurement indicates that electromagnetic modeling will play an important role in material characterizations.

REFERENCES

[1] G. Birnbaum and J. Franeau, "Measurement of the dielectric constant and loss of solids and liquids by a cavity perturbation method," *J. Appl. Phys.*, vol. 20, 1949, pp. 817–818.
[2] W. B. Weir, "Automatic measurement of complex dielectric constant and permeability at microwave frequencies," *Proc. IEEE*, vol. 62, pp 33–36, Jan. 1974.
[3] J. Ness, "Broad-band permittivity measurements using the semi-automatic network analyzer," *IEEE Trans. Microwave Theory Tech.*, vol. MTT-33, pp. 1222–1226, Nov. 1985.
[4] W. Barry, "A broad-band, automated, stripline technique for the simultaneous measurement of complex permittivity and permeability," *IEEE Trans. Microwave Theory Tech.*, vol. MTT-34, pp. 80–84, Jan. 1986.
[5] N. Belhadj-Tahar, A. Fourrier-Lamer, and H. De Chanterac, "Broad-band simultaneous measurement of complex permittivity and permeability using a coaxial discontinuity," *IEEE Trans. Microwave Theory Tech.*, vol MTT-38, pp. 1–7, Jan. 1990.
[6] H. Jin and R. Vahldieck, "The frequency-domain TLM method—A new concept," *IEEE Trans. Microwave Theory and Tech* vol. MTT-40, pp 2207–2218, Dec. 1992
[7] J. Huang, R. Vahldieck, and H. Jin, "Fast frequency-domain TLM analysis of 3D circuit discontinuities," in *9th Annual Review of Progress in Applied Computational Electromagnetics Symp.*, Monterey, CA, Mar. 22–26, 1993.
[8] J. Abdulnour, C. Akyel, and K. Wu, "A generic approach for permittivity measurement of dielectric materials using a discontinuity in a rectangular waveguide or a microstrip line," *IEEE Trans. Microwave Theory Tech.* MTT-43, pp. 1060–1066, May 1995
[9] J. Huang, R. Vahldieck, and H Jin, "Microstrip discontinuities on cylindrical surfaces," in *1993 IEEE MTT-S Int. Microwave Symp. Dig.*, pp. 1299–1302.
[10] P. B. Johns, "A symmetrical condensed node for the TLM method," *IEEE Trans. Microwave Theory Tech.*, vol. MTT-35, pp. 370–377, Apr. 1987.
[11] R. Scaramuzza and A. J. Lowery, "Hybrid symmetrical condensed node for the TLM method," *Electron. Lett.*, vol. 28, no. 23, pp 1947–1949, Nov. 1990
[12] R. Allen and M J. Clark, "Application of the symmetrical transmission line matrix method to the cold modeling of magnetrons," *Int. J. Numerical Modeling*, vol. 1, pp. 61–70, 1988.
[13] J. Huang, "Frequency-domain TLM method and its applications to electromagnetic analysis," *Ph.D. Dissertation,* Univ. of Victoria, BC, Canada, 1995.

Jifu Huang received the B. Eng. and M. Eng. degrees in radio engineering from Nanjing Institute of Technology (now Southeast University), Nanjing, China, in 1982 and 1987, respectively, and the Ph. D degree in electrical and computer engineering from University of Victoria, Canada, in 1995.

He joined the faculty of radio engineering at Southeast University in 1982, where he worked as a Research and Teaching Assistant, and from 1987 to 1991 as a Lecturer. From 1991 to 1994, he was a Research Assistant in the Department of Electrical and Computer Engineering at the University of Victoria, B.C., Canada. From 1994 to 1995, he worked as a postdoctoral fellow at the Research Center for Advanced Microwave and Space Electronics at the Ecole Polytechnique of Montreal, Canada. Subsequently, he joined the Harris Farinon Canada as a Senior RF Engineer responsible for R&D of RF and microwave communication products.

Ke Wu (M'87–SM'92) for a photograph and biography, see this issue, p. 759.

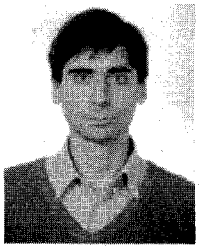

Patrick Morin was born in St.-Eustache, Canada, in 1969. He received the B.Ing. degree in electrical engineering from the École Polytechnique de Montréal in 1993. He is now working for the M.Sc.A. degree in numerical modeling of microwave passive devices at Centre de Recherche Polygrames from Polytechnique de Montréal.

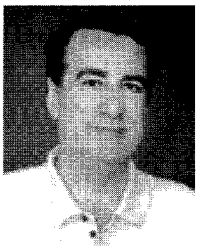

Cevdet Akyel (S'74–M'88) received the B.Sc. degree in electrical engineering from the Technical University of Istanbul in 1971. He received the M.Sc.A. and D.Sc.A. degrees in microwave measurement techniques from École Polytechique, Université de Montréal in 1975 and 1980, respectively.

He was a System Engineer with the Northern Telecom Company in Montréal from 1974 to 1976. He held the position of NSERC Research Fellow at École Polytechnique from 1980 to 1985 where he was appointed Professor in material/wave interactions in electromagnetics. His main interests in microwaves cover instrumentations, permittivity and permeability measurements, automated techniques, low power sensors, and high power microwave applicators.